T-FETI Based Algorithm for 3D Contact Problems with Orthotropic Friction

Jaroslav Haslinger and Radek Kučera

Abstract The contribution deals with contact problems for two elastic bodies with an orthotropic Coulomb friction law. To find a solution, the method of successive approximations is combined with the augmented Lagrangian algorithm. As the problem is discretized by the T-FETI domain decomposition method, the algorithm is scalable, i.e., the number of iterations needed to achieve a prescribed accuracy can be independent of the mesh norms. The scalability is experimentally demonstrated on a model example.

1 Introduction

Contact problems represent a special branch of mechanics of solids whose goal is to find an equilibrium state of deformable bodies being in a mutual contact. Due to non-penetration and friction conditions, problems we have to solve are highly nonlinear. For linearly elastic materials obeying the Hook law for small deformations, a linearization of the non-penetration conditions (see [14, 12]) leads to a convex set of kinematically admissible displacements (geometrical nonlinearity). Another nonlinearity originates from the presence of friction. In the simplest case with an à-priori given slip bound (Tresca model), the mathematical model is represented by a variational inequality of the second kind (see [8, 12]). This model is however too simple since the non-penetration and friction phenomena are decoupled. For this reason more realistic models of friction have to be used and the Coulomb friction law is the classical one. The slip bound prescribed in Tresca model is now replaced by the product of a coefficient of friction $\mathscr{F}$ and the norm of the normal contact force. The coupling of unilateral and friction conditions leads to the so-called implicit variational inequality (in terms of displacements) or to a quasivariational inequality (in terms of contact stresses) ([14, 12]). Due to material or contact surface properties

Centre of Excellence IT4I, VŠB-TU Ostrava, 17. listopadu 15, 70833 Ostrava, Czech Republic, e-mail: hasling@karlin.mff.cuni.cz (JH), radek.kucera@vsb.cz (RK)

it may happen that the effect of friction is directionally dependent. A discretization and numerical realization of 3D contact problems with orthotropic Coulomb friction characterized by two coefficients of friction $\mathscr{F}_1$ and $\mathscr{F}_2$ in two mutually orthogonal directions have been presented in [13].

This paper is devoted to the mathematical analysis of algebraic counterparts of the discretized contact problem with orthotropic Tresca model of friction. Its dual formulation (in terms of the contact stresses) leads to a convex programming problem: a minimization of a quadratic function over a convex set given by simple constraints for the discrete normal contact stress and separable quadratic (ellipsoidal) constraints for the discrete tangential (friction) forces. This minimization can be performed by the algorithm proposed in [18]. To increase the efficiency of the computational process we apply a variant of the FETI domain decomposition method which introduces (additionally to the original setting) also equality constraints by means of which the solutions on the individual sub-domains are glued together.The resulting minimization problem is realized by the augmented Lagrangian method ([4]) in which the algorithm from [18] is used repeatedly. To solve contact problems with orthotropic Coulomb friction, the augmented Lagrangian method is combined with the method of successive approximations.

The properties of the FETI domain decomposition method ([7]) play the key role in our analysis. There are two main benefits of this approach. Firstly, the stiffness matrix has a block diagonal structure. This enables us to handle the blocks in parallel. Secondly, the spectrum of all blocks and, consequently of the whole stiffness matrix, lies within an interval in $\mathbb{R}^1_+$ which (under additional assumptions on the used partitions) does not dependent on the mesh norms. It is well-known that convergence of conjugate gradient type methods depends on the spectrum of the matrix ([9, 5, 18]). Therefore the number of iterations needed to get a solution with a given accuracy can be independent of the mesh norms, as well. This property is known as the *scalability* of the method ([2]). One of reasons for developing variants to the original FETI method is the effort to increase the efficiency of operations with a generalized inverse (or inverse itself) to the stiffness matrix ([6, 15, 3]). In this paper we shall use the so-called total FETI (T-FETI) method ([3]) in which also the Dirichlet boundary conditions are enforced by the Lagrange multipliers. The advantage of this variant is the fact that all sub-bodies can be treated as floating structures with six rigid body modes. Thus the kernel space of the stiffness matrix can be identified directly without any computation and, consequently, the Moore-Penrose inverse is easily available. In this paper we give the analysis of the T-FETI method for solving contact problems with orthotropic friction in which the properties of the Moore-Penrose inverse play a fundamental role.

The paper is organized as follows: Section 2 deals with the continuous setting of contact problems with orthotropic Coulomb friction. First we present its classical formulation. The week formulation is defined by means of the fixed-point approach. A contact problem with orthotropic Tresca friction serves as one iterative step in the method of successive approximations. In Section 3 we introduce the finite element approximation of this auxiliary problem based on the T-FETI domain decomposition method. The displacements are approximated by linear functions on tetrahedrons.

In Section 4 we analyze the algebraic formulation of the discretized problem. It is shown that the spectrum of the penalized dual Hessian lies in an interval whose bounds are independent of the mesh norms provided that the ratio between the domain decomposition norm H and the finite element norm h is bounded. Using these results one can prove that the algorithm presented in Section 5 finds the solution by $O(1)$ matrix-vector multiplications independently of the mesh norms. Finally in Section 6 we present results of numerical experiments and in Section 7 we give concluding remarks.

2 Problem Formulation

Let us consider two elastic bodies represented by two non-overlapping polyhedral domains $\Omega^k \subset \mathbb{R}^3$ with the boundaries $\partial\Omega^k$, $k = 1,2$. Each boundary consists of three non-empty disjoint parts Γ_u^k, Γ_p^k, and Γ_c^k open in $\partial\Omega^k$, so that $\partial\Omega^k = \overline{\Gamma}_u^k \cup \overline{\Gamma}_p^k \cup \overline{\Gamma}_c^k$. The zero displacements are prescribed on Γ_u^k while surface tractions of density p^k act on Γ_p^k. On the *contact interfaces* given by Γ_c^1 and Γ_c^2 we consider contact conditions: the non-penetration of the bodies, the transmission of the contact stresses, and the effect of orthotropic Coulomb friction. Finally we suppose that each body Ω^k is subject to volume forces of density f^k (see Figure 1 for our model problem).

We seek displacement fields u^k in Ω^k satisfying the *equilibrium equations* and the *Dirichlet and Neumann boundary conditions*:

$$\left.\begin{aligned} \operatorname{div}\sigma^k + f^k &= 0 \ \text{ in } \ \Omega^k, \\ u^k &= 0 \ \text{ on } \ \Gamma_u^k, \\ \sigma^k n^k - p^k &= 0 \ \text{ on } \ \Gamma_p^k, \end{aligned}\right\} \quad k = 1,2, \tag{1}$$

where $\sigma^k := \sigma(u^k)$ is the stress tensor in Ω^k and n^k stands for the unit outward normal vector to $\partial\Omega^k$, $k = 1,2$. Stress tensors are related to linearized strain tensors $\varepsilon^k := \varepsilon(u^k) = 1/2(\nabla u^k + \nabla^\top u^k)$ by Hooke's law for linear isotropic materials:

$$\sigma^k := \lambda^k \operatorname{tr}(\varepsilon^k) I + 2\mu^k \varepsilon^k \quad \text{in} \quad \Omega^k,$$

where "tr" denotes the trace of matrices, $I \in \mathbb{R}^{3\times 3}$ is the identity matrix, and $\lambda^k, \mu^k > 0$ are the Lamè constants characterizing material properties of the bodies.

To formulate the contact conditions we introduce a predefined one-to-one transfer mapping $\chi : \Gamma_c^1 \mapsto \Gamma_c^2$ by means of which we define the initial distance between the contact surfaces at $x \in \Gamma_c^1$ as $d(x) := \|\chi(x) - x\|$ and the critical direction $\nu(x) := (\chi(x) - x)/d(x)$ if $d(x) \neq 0$, or $\nu(x) := n^1(x)$ if $d(x) = 0$. Here and in what follows, $\|\cdot\|$ stands for the Euclidean norm of a vector. The non-penetration conditions read as follows:

$$u_\nu - d \leq 0, \ \sigma_\nu \leq 0, \ \sigma_\nu(u_\nu - d) = 0 \quad \text{on} \quad \Gamma_c^1, \tag{2}$$

where $u_\nu(x) := (u^1(x) - u^2(\chi(x)))^\top \nu(x)$ is the relative contact displacement and $\sigma_\nu(x) := \nu(x)^\top \sigma^1(x) n^1(x)$ is the contact stress at $x \in \Gamma_c^1$, both in the direction of $\nu(x)$.

Further we require the *transmission of the contact stresses*:

$$\sigma^1 \nu = (\sigma^2 \circ \chi)\nu \quad \text{on } \Gamma_c^1, \tag{3}$$

where $(\sigma^2 \circ \chi)(x) := \sigma^2(\chi(x))$ at $x \in \Gamma_c^1$.

Finally let $t_1 := t_1(x)$, $t_2 := t_2(x)$ be two vectors orthogonal to $\nu := \nu(x)$ and such that the triplet $\{\nu, t_1, t_2\}$ is an orthonormal basis in $\mathbb{R}^3$ with the origin at $x \in \Gamma_c^1$, which is piecewise smooth on Γ_c^1. By $\mathscr{F}_1 := \mathscr{F}_1(x)$, $\mathscr{F}_2 := \mathscr{F}_2(x)$ we denote positive coefficients of friction in the directions t_1, t_2, respectively, and set

$$\mathscr{F} := \mathscr{F}(x) = \begin{pmatrix} \mathscr{F}_1(x) & 0 \\ 0 & \mathscr{F}_2(x) \end{pmatrix} \in \mathbb{R}^{2\times 2}, \; x \in \Gamma_c^1.$$

The *orthotropic Coulomb friction law* reads as follows:

$$\left.\begin{aligned} u_t(x) = 0 &\Longrightarrow \|\mathscr{F}^{-1}\sigma_t(x)\| \le -\sigma_\nu(x) \\ u_t(x) \ne 0 &\Longrightarrow \mathscr{F}^{-1}\sigma_t(x) = \sigma_\nu(x)\frac{\mathscr{F}u_t(x)}{\|\mathscr{F}u_t(x)\|} \end{aligned}\right\} \quad x \in \Gamma_c^1, \tag{4}$$

where $u_t := (u_{t_1}, u_{t_2})^\top$ and $\sigma_t := (\sigma_{t_1}, \sigma_{t_2})^\top$ is the relative tangential contact displacement and the tangential contact stress at $x \in \Gamma_c^1$ with the components $u_{t_i}(x) := (u^1(x) - u^2(\chi(x)))^\top t_i(x)$ and $\sigma_{t_i}(x) := t_i(x)^\top \sigma^1(x) n^1(x)$, $i = 1,2$, respectively.

The classical solution of the *contact problem with orthotropic Coulomb friction* is a pair $u := (u^1, u^2)$ of the displacement fields u^k in Ω^k, $k = 1,2$, satisfying (1)–(4). Let us note that the weak formulation of this problem leads to the implicit variational inequality [10]. To overcome this difficulty we replace (4) by the *orthotropic Tresca friction law*:

$$\left.\begin{aligned} u_t(x) = 0 &\Longrightarrow \|\mathscr{F}^{-1}\sigma_t(x)\| \le g(x) \\ u_t(x) \ne 0 &\Longrightarrow -\mathscr{F}^{-1}\sigma_t(x) = g(x)\frac{\mathscr{F}u_t(x)}{\|\mathscr{F}u_t(x)\|} \end{aligned}\right\} \quad x \in \Gamma_c^1, \tag{5}$$

where g is the à-priori given positive *slip bound* on Γ_c^1. The *contact problem with orthotropic Tresca friction* is described by (1)–(3), and (5). Before giving its weak formulation we introduce notation.

Let us denote:

$$\begin{aligned} \mathbb{V} &= \{w := (w^1, w^2) \in (H^1(\Omega^1))^3 \times (H^1(\Omega^2))^3 |\; w^k = 0 \text{ on } \Gamma_u^k,\; k = 1,2\}, \\ \mathbb{K} &= \{w \in \mathbb{V} |\; w_\nu - d \le 0 \text{ on } \Gamma_c^1\}, \\ X_\nu &= \{\varphi \in L^2(\Gamma_c^1) |\; \exists w \in \mathbb{V} :\; \varphi = w_\nu \text{ on } \Gamma_c^1\}, \\ X_{\nu+} &= \{\varphi \in X_\nu |\; \varphi \ge 0 \text{ on } \Gamma_c^1\}. \end{aligned}$$

The symbol X_ν' stands for the dual of X_ν and $X_{\nu+}'$ for the cone of all non-negative elements of X_ν'. The duality pairing between X_ν' and X_ν will be denoted by $\langle\cdot,\cdot\rangle$, in what follows. We will suppose that $\|\mathscr{F}w_t\| \in X_\nu$ so that $\langle g, \|\mathscr{F}w_t\|\rangle$ is well defined for any $g \in X_\nu'$ and $w \in \mathbb{V}$. Moreover we assume that $f^k \in (L^2(\Omega^k))^3$, $p^k \in (L^2(\Gamma_p^k))^3$, $k = 1,2$, $d \in X_{\nu+}$. Finally $\mathscr{F}_i$ will be sufficiently smooth and $\mathscr{F}_{\min} \le \mathscr{F}_i \le \mathscr{F}_{\max}$ on Γ_c^1, $i = 1,2$, with $0 < \mathscr{F}_{\min} < \mathscr{F}_{\max}$.

Let $g \in X_{\nu+}'$ be given. By the *weak solution* of the contact problem with orthotropic Tresca friction we call $u := u(g) \in \mathbb{K}$ satisfying the variational inequality of the second kind:

$$a(u, w-u) + \langle g, \|\mathscr{F}w_t\| - \|\mathscr{F}u_t\|\rangle \ge b(w-u) \quad \forall w \in \mathbb{K}, \tag{6}$$

where

$$a(u,w) = \sum_{k=1}^{2} \int_{\Omega^k} \sigma(u^k) : \varepsilon(w^k)\,\mathrm{d}x,$$
$$b(w) = \sum_{k=1}^{2} \Big(\int_{\Omega^k} (f^k)^\top w^k\,\mathrm{d}x + \int_{\Gamma_p^k} (p^k)^\top w^k\,\mathrm{d}s \Big).$$

It is well-known [10] that (6) is equivalent to the minimization problem:

$$\left.\begin{array}{l} \textit{Find } u := u(g) \in \mathbb{K} \textit{ such that} \\ J_g(u) \le J_g(w) \quad \forall w \in \mathbb{K}, \end{array}\right\} \tag{$\mathscr{P}(g)$}$$

where $J_g(w) = \frac{1}{2}a(w,w) - b(w) + \langle g, \|\mathscr{F}w_t\|\rangle$. Let us note that the bilinear form $a(\cdot,\cdot)$ is symmetric, coercive, and bounded on $\mathbb{V}\times\mathbb{V}$.

Since $(\mathscr{P}(g))$ has a unique solution and assuming that $-\sigma_\nu(u(g)) \in X_{\nu+}'$ for every $g \in X_{\nu+}'$, one can define the mapping $\Psi : X_{\nu+}' \mapsto X_{\nu+}'$ by:

$$\Psi : g \mapsto -\sigma_\nu(u(g)), \quad g \in X_{\nu+}', \tag{7}$$

where $\sigma_\nu(u(g))$ is the contact stress on Γ_c^1 in the direction of ν associated with the solution $u(g)$ to $(\mathscr{P}(g))$. By a *weak solution* to the contact problem with orthotropic Coulomb friction we call any $u \in \mathbb{K}$ such that

$$\Psi(-\sigma_\nu(u)) = -\sigma_\nu(u), \tag{$\mathscr{P}$}$$

i.e., $-\sigma_\nu(u)$ is a fixed point of Ψ in $X_{\nu+}'$.

Since the method of successive approximations will be the main tool for solving $(\mathscr{P})$, we will confine ourselves to the individual iterative step represented by $(\mathscr{P}(g))$. In the next section we will discretize $(\mathscr{P}(g))$ using the T-FETI domain decomposition method under the additional assumption that $g \in L^2_+(\Gamma_c^1)$. In such a case the duality pairing $\langle\cdot,\cdot\rangle$ is represented by the $L^2(\Gamma_c^1)$-scalar product so that the frictional term in $(\mathscr{P}(g))$ can be approximated by a suitable cubature formula.

3 Domain Decomposition and Discretization

In this section we introduce a finite element approximation of $(\mathscr{P}(g))$ based on the T-FETI domain decomposition method [3]. The continuous setting of this domain decomposition variant applied to contact problems is described in [13]. Here we recall the main ides leading to the algebraic formulation.

Let $\{\Omega_H^{ki}\}_{i=1}^{s_k}$, $k=1,2$, be a decomposition of Ω^k into s_k *polyhedral* subdomains Ω_H^{ki} with the Lipschitz boundaries $\partial\Omega_H^{ki}$ such that $\overline{\Omega}^k = \bigcup_{i=1}^{s_k} \overline{\Omega}_H^{ki}$, $\Omega_H^{ki} \cap \Omega_H^{kj} = \emptyset$, $i \neq j$. The symbol H stands for the *decomposition parameter* that is the diameter of the largest subdomain. In addition we will suppose that these decompositions are compatible with the partition of $\partial\Omega^k$ into Γ_u^k, Γ_p^k, and Γ_c^k, $k=1,2$. We say that Γ_{ij}^k is a common interface between Ω_H^{ki} and Ω_H^{kj}, $i \neq j$, iff $meas_2 \Gamma_{ij}^k > 0$, where $\Gamma_{ij}^k := \partial\Omega_H^{ki} \cap \partial\Omega_H^{kj}$ and $meas_2$ stands for the two-dimensional Lebesgue measure of a set. To identify common interfaces we introduce the index sets:

$$\mathscr{I}^k := \{(i,j) |\ 1 \leq i < j \leq s_k,\ meas_2(\Gamma_{ij}^k) > 0\}, \quad k=1,2.$$

A regular partition of $\overline{\Omega}_H^{ki}$ into tetrahedrons will be denoted by $\mathscr{T}_{Hh}^{ki}$, where h is the *discretization parameter* that is the diameter of the largest tetrahedron. We will assume that the nodes of $\mathscr{T}_{Hh}^{ki}$ and $\mathscr{T}_{Hh}^{kj}$ coincide on the common interface between Ω_H^{ki} and Ω_H^{kj}. Moreover $\mathscr{T}_{Hh}^{ki}$ will be consistent with $\Gamma_u^k \cap \partial\Omega_H^{ki}$, $\Gamma_p^k \cap \partial\Omega_H^{ki}$, and $\Gamma_c^k \cap \partial\Omega_H^{ki}$, $k=1,2$. On $\mathscr{T}_{Hh}^{ki}$ we define the finite element space:

$$\mathbb{V}_{Hh}^{ki} := \{w_{Hh}^{ki} \in (C(\overline{\Omega}^{ki}))^3 : w_{Hh|T}^{ki} \in (P_1(T))^3 \text{ for all } T \in \mathscr{T}_{Hh}^{ki}\},$$

where $P_1(T)$ denotes the set of all polynomials of degree less or equal one on T. Let $n_{ki} := \dim \mathbb{V}_{Hh}^{ki}$. Finally we introduce the product space:

$$\mathbb{V}_{Hh} := \prod_{i=1}^{s_1} \mathbb{V}_{Hh}^{1i} \times \prod_{i=1}^{s_2} \mathbb{V}_{Hh}^{2i}, \quad w_{Hh} := (w_{Hh}^1, w_{Hh}^2) \in \mathbb{V}_{Hh}.$$

Let us note that the Dirichlet boundary conditions are not included in the definition of $\mathbb{V}_{Hh}$ and also the non-zero jumps $[w_{Hh}^k]_{ij} := (w_{Hh}^{ki} - w_{Hh}^{kj})_{|\Gamma_{ij}^k}$ are allowed on the interfaces Γ_{ij}^k, $(i,j) \in \mathscr{I}^k$, $k=1,2$, for $w_{Hh} \in \mathbb{V}_{Hh}$. Thus $n := \dim \mathbb{V}_{Hh} = \sum_{k=1}^2 \sum_{i=1}^{s_k} n_{ik}$. As we shall see later, this definition of $\mathbb{V}_{Hh}$ simplifies considerably properties of the stiffness matrix since it enables us to identify easily its kernel-space.

In order to define the discretization $\mathbb{K}_{Hh}$ of $\mathbb{K}$ we introduce the index set

$$\mathscr{I}^c := \{i |\ 1 \leq i \leq s_1,\ meas_2(\Gamma_{ci}^1) > 0,\ \Gamma_{ci}^1 := \partial\Omega_H^{1i} \cap \Gamma_c^1\}.$$

Then $\overline{\Gamma}_c^1 = \bigcup_{i\in\mathscr{I}^c} \overline{\Gamma}_{ci}^1$. Let $\mathscr{N}_i := \{x_{iq}^1\}_{q=1}^{m_i}$, $i \in \mathscr{I}^c$, be the set of all contact nodes of $\mathscr{T}_{Hh}^{1i}$, i.e., x_{iq}^1 is the vertex of a tetrahedron $T \in \mathscr{T}_{Hh}^{1i}$ such that $x_{qi}^1 \in \overline{\Gamma}_{ci}^1 \setminus \overline{\Gamma}_u^1$. The admissible set $\mathbb{K}_{Hh}$ is defined as follows:

$$\mathbb{K}_{Hh} := \{w_{Hh} \in \mathbb{V}_{Hh} |\ w_{Hh,\nu}(x_{iq}^1) - d(x_{iq}^1) \le 0\ \ \forall q = 1,\dots,m_i,\ \forall i \in \mathscr{I}^c,$$
$$[w_{Hh}^k]_{ij} = 0\ \ \forall (i,j) \in \mathscr{I}^k,\ w_{Hh}^k = 0 \text{ on } \Gamma_u^k,\ k = 1,2\},$$

i.e., $\mathbb{K}_{Hh}$ contains all continuous piecewise-linear vector functions in Ω^1, Ω^2 satisfying the homogeneous Dirichlet condition on $\Gamma_u^1 \cup \Gamma_u^2$ and the non-penetration condition at all contact nodes. The set $\mathbb{K}_{Hh}$ is an *external* approximation of $\mathbb{K}$, i.e., $\mathbb{K}_{Hh} \not\subseteq \mathbb{K}$, in general.

To approximate the frictional term we associate with any $x_{iq}^1 \in \mathscr{N}_i$ an element $R_{iq} \subset \overline{\Gamma}_{ci}^1$, $meas_2(R_{iq}) > 0$, such that $\overline{\Gamma}_{ci}^1 = \bigcup_{q=1}^{m_i} \overline{R}_{iq}$. As mentioned above, the duality pairing $\langle\cdot,\cdot\rangle$ is replaced by the $L^2(\Gamma_c^1)$-scalar so that the frictional term can be approximated as follows:

$$\langle g, \|\mathscr{F} w_{Hh,t}\|\rangle \approx \sum_{i\in\mathscr{I}^c} \sum_{q=1}^{m_i} g_{iq} \|\mathscr{F} w_{Hh,t}(x_{iq}^1)\| =: j_{Hh}(w_{Hh}), \quad w_{Hh} \in \mathbb{V}_{Hh},$$

where $g_{iq} := \int_{R_{iq}} g\,\mathrm{d}s$.

The finite element approximation of $(\mathscr{P}(g))$ reads as follows:

$$\left.\begin{array}{l} \text{Find } u_{Hh} := u_{Hh}(g) \in \mathbb{K}_{Hh} \text{ such that} \\ J_{g,Hh}(u_{Hh}) \le J_{g,Hh}(w_{Hh}) \quad \forall w_{Hh} \in \mathbb{K}_{Hh}, \end{array}\right\} \qquad (\mathscr{P}_{Hh}(g))$$

where $J_{g,Hh}(w_{Hh}) := \dfrac{1}{2} a(w_{Hh}, w_{Hh}) - b(w_{Hh}) + j_{Hh}(w_{Hh})$. The algebraic counterpart of $(\mathscr{P}_{Hh}(g))$ will be discussed in the next section.

4 Algebraic Formulations

First of all we introduce notation. Let $\mathbb{U} \subseteq \mathbb{R}^q$ be a subspace. The kernel-space and the image-space of any matrix $\mathbf{M} \in \mathbb{R}^{p\times q}$ on $\mathbb{U}$ will be denoted by $Ker(\mathbf{M}|\mathbb{U})$ and $Im(\mathbf{M}|\mathbb{U})$, respectively. If $\mathbf{M}$ is symmetric, positive semi-definite (with $p = q$) on $\mathbb{U}$, we will denote the largest eigenvalue on $\mathbb{U}$ by $\lambda_{\max}(\mathbf{M}|\mathbb{U})$ and the smallest eigenvalue on $\mathbb{U}$ by $\lambda_{\min}(\mathbf{M}|\mathbb{U})$. The spectral condition number of $\mathbf{M}$ on $\mathbb{U}$ is defined by

$$\kappa(\mathbf{M}|\mathbb{U}) := \frac{\lambda_{\max}(\mathbf{M}|\mathbb{U})}{\lambda_{\min}(\mathbf{M}|\mathbb{U})}.$$

Moreover when $\mathbb{U} = \mathbb{R}^q$, we simply write $Ker\,\mathbf{M} := Ker(\mathbf{M}|\mathbb{U})$, $Im\,\mathbf{M} := Im(\mathbf{M}|\mathbb{U})$, $\lambda_{\min}(\mathbf{M}) := \lambda_{\min}(\mathbf{M}|\mathbb{U})$, $\lambda_{\max}(\mathbf{M}) := \lambda_{\max}(\mathbf{M}|\mathbb{U})$, and $\kappa(\mathbf{M}) := \kappa(\mathbf{M}|\mathbb{U})$. Let us note

that $0 < \lambda_{\min}(\mathbf{M}|Im\,\mathbf{M})$, $\lambda_{\max}(\mathbf{M}|Im\,\mathbf{M}) = \lambda_{\max}(\mathbf{M})$, and $\kappa(\mathbf{M}|Im\,\mathbf{M}) < +\infty$, if $\mathbf{M}$ is a non-zero matrix.

4.1 Primal Formulation

Problem $(\mathscr{P}_{Hh}(g))$ can be written in the following algebraic form:

$$\textit{Find } \mathbf{u} \in K \textit{ such that } J_{\mathbf{g}}(\mathbf{u}) = \min_{\mathbf{v}\in K} J_{\mathbf{g}}(\mathbf{v}) \qquad (\mathscr{P}_{Hh}(\mathbf{g}))$$

with

$$J_{\mathbf{g}}(\mathbf{v}) := \frac{1}{2}\mathbf{v}^\top \mathbf{K}\mathbf{v} - \mathbf{v}^\top \mathbf{f} + \sum_{r=1}^{m} g_r \|\mathscr{F}_r(\mathbf{T}_{1r}\mathbf{v}, \mathbf{T}_{2r}\mathbf{v})^\top\|,$$
$$K := \{\mathbf{v} \in \mathbb{R}^n : \mathbf{N}\mathbf{v} - \mathbf{d} \le \mathbf{0},\ \mathbf{B}_e\mathbf{v} = \mathbf{0},\ \mathbf{B}_d\mathbf{v} = \mathbf{0}\},$$

where $\mathbf{v} \in \mathbb{R}^n$ is the nodal displacement vector, $\mathbf{K} \in \mathbb{R}^{n\times n}$ denotes the symmetric, positive semi-definite stiffness matrix, $\mathbf{f} \in \mathbb{R}^n$ is the load vector, and $\mathbf{N} \in \mathbb{R}^{m\times n}$, $m := \sum_{i\in\mathscr{J}^c} m_i$, is the matrix whose the r-th row $\mathbf{N}_r$ projects the displacement vector at a contact node x^1_{iq} to the direction $\nu(x^1_{iq})$. Further $\mathbf{B}_e \in \mathbb{R}^{m_e\times n}$, $\mathbf{B}_d \in \mathbb{R}^{m_d\times n}$ are the matrices representing the jumps across the inter-element boundaries and realizing the Dirichlet boundary conditions, respectively. Finally $(\mathbf{T}_{1r}\mathbf{v}, \mathbf{T}_{2r}\mathbf{v})^\top \in \mathbb{R}^2$, $r = 1,\dots,m$, is the vector of the tangential displacements at a contact node x^1_{iq}, where $\mathbf{T}_{1r}, \mathbf{T}_{2r}$ denotes the r-th row of the matrix $\mathbf{T}_1$ and $\mathbf{T}_2 \in \mathbb{R}^{m\times n}$, respectively. In other words $\mathbf{T}_{1r}$, $\mathbf{T}_{2r}$ projects the displacement vector at x^1_{iq} to the direction $t_1(x^1_{iq})$ and $t_2(x^1_{iq})$, respectively. This notation requires a one-to-one correspondence between the global indices $r := r(i,q)$ and the local indices i,q. Thus $\mathscr{F}_r := \mathscr{F}(x^1_{iq}) \in \mathbb{R}^{2\times 2}$ and $\mathbf{g}, \mathbf{d} \in \mathbb{R}^m$ have the components $g_r := g_{iq}$, $d_r := d(x^1_{iq})$.

Remark 1. In general, the rows of the matrices $\mathbf{N}, \mathbf{T}_1, \mathbf{T}_2, \mathbf{B}_e, \mathbf{B}_d$ are linearly dependent that is not acceptable for the algorithm discussed below. Therefore redundant rows will be eliminated and the resulting full row-rank matrices will be denoted by the same symbols.

The stiffness matrix $\mathbf{K}$ is block diagonal:

$$\mathbf{K} = diag(\mathbf{K}^{11}, \dots, \mathbf{K}^{1s_1}, \mathbf{K}^{21}, \dots, \mathbf{K}^{2s_1}),$$

where $\mathbf{K}^{ki}$ are the stiffness matrices on the subdomains Ω^{ki}, $i = 1,\dots,s_k$, $k = 1,2$. As we use the T-FETI domain decomposition method, the homogenous traction boundary conditions on $\partial\Omega^{ki}$ are assumed when assembling $\mathbf{K}^{ki}$. Therefore each $\mathbf{K}^{ki}$ can be understood as the stiffness matrix of the floating body Ω^{ki} with six rigid body modes. A mechanical background of the problem enables us to identify the rigid body modes directly without any computation [3]. Consequently one can assemble the orthogonal matrices $\mathbf{R}^{ki} \in \mathbb{R}^{n_{ki}\times 6}$ whose columns span $Ker\,\mathbf{K}^{ki}$. The matrix $\mathbf{R} \in \mathbb{R}^{n\times 6(s_1+s_2)}$ spanning $Ker\,\mathbf{K}$ exhibits the following block diagonal structure:

$$\mathbf{R} = diag(\mathbf{R}^{11}, \ldots, \mathbf{R}^{1s_1}, \mathbf{R}^{21}, \ldots, \mathbf{R}^{2s_1}).$$

Assumption 1. Next we will assume that there exist constants $c_1 > 0$, $c_2 > 0$ independent of the decomposition and discretization parameters H and h, respectively, such that

$$c_1 \frac{h}{H} \leq \lambda_{\min}(\mathbf{K}^{ki} | Im\, \mathbf{K}^{ki}) \quad \text{and} \quad \lambda_{\max}(\mathbf{K}^{ki}) \leq c_2 \frac{H}{h}$$

for $i = 1, \ldots, s_k$, $k = 1, 2$.

Lemma 1. *It holds:*

$$c_1 \frac{h}{H} \leq \lambda_{\min}(\mathbf{K} | Im\, \mathbf{K}) \quad \textit{and} \quad \lambda_{\max}(\mathbf{K}) \leq c_2 \frac{H}{h}. \tag{8}$$

Proof. It follows from the fact that $\mathbf{K}$ is block diagonal with the blocks $\mathbf{K}^{ki}$. □

As $\mathbf{K}$ is positive semi-definite, one can decompose it (per blocks) by the generalized Cholesky factorization [9] from which the generalized inverse $\mathbf{K}^+$ satisfying $\mathbf{K} = \mathbf{K}\mathbf{K}^+\mathbf{K}$ is easily available. Unfortunately such $\mathbf{K}^+$ may considerably change the spectral condition number of $\mathbf{K}$. Therefore we prefer to use the Moore-Penrose inverse that will be denoted by $\mathbf{K}^\dagger$ in what it follows. The next lemma shows how to obtain $\mathbf{K}^\dagger$ from $\mathbf{K}^+$ and $\mathbf{R}$.

Theorem 1. *Let $\mathbf{K}^+$ be an arbitrary generalized inverse to $\mathbf{K}$ and let the columns of $\mathbf{R}$ form an orthogonal basis of $Ker\,\mathbf{K}$. Then the Moore-Penrose inverse is given by*

$$\mathbf{K}^\dagger = (\mathbf{I} - \mathbf{R}\mathbf{R}^\top)\mathbf{K}^+(\mathbf{I} - \mathbf{R}\mathbf{R}^\top). \tag{9}$$

Moreover it holds:

$$c_2^{-1} \frac{h}{H} \leq \lambda_{\min}(\mathbf{K}^\dagger | Im\, \mathbf{K}) \quad \textit{and} \quad \lambda_{\max}(\mathbf{K}^\dagger | Im\, \mathbf{K}) \leq c_1^{-1} \frac{H}{h}. \tag{10}$$

Proof. The Moore-Penrose inverse to $\mathbf{K}$ is fully characterized by the following three conditions:

$$\mathbf{K} = \mathbf{K}\mathbf{K}^\dagger\mathbf{K}, \quad Im\,\mathbf{K}^\dagger = Im\,\mathbf{K}^\top, \quad Ker\,\mathbf{K}^\dagger = Ker\,\mathbf{K}^\top. \tag{11}$$

Since $\mathbf{K}$ is symmetric and $\mathbf{I} - \mathbf{R}\mathbf{R}^\top$ is the orthogonal projector on $Im\,\mathbf{K}$, one can verify that $\mathbf{K}^\dagger$ given by (9) fulfils (11). Further the singular-value decomposition of $\mathbf{K}$ yields

$$\lambda_{\min}(\mathbf{K}^\dagger | Im\, \mathbf{K}) = \lambda_{\max}(\mathbf{K})^{-1} \quad \text{and} \quad \lambda_{\max}(\mathbf{K}^\dagger | Im\, \mathbf{K}) = \lambda_{\min}(\mathbf{K} | Im\, \mathbf{K})^{-1}$$

so that (10) follows from (8) (see [19] for more details). □

4.2 Dual Formulation

The primal formulation $(\mathscr{P}_{Hh}(\mathbf{g}))$ is not suitable for direct computations as the constraints in K can be hardly handled for large-scale problems. Moreover the functional $J_{\mathbf{g}}$ is non-differentiable due to the frictional term. In order to overcome these difficulties, we will use the dual formulation of $(\mathscr{P}_{Hh}(\mathbf{g}))$.

First we show how to regularize the non-differentiable term in $(\mathscr{P}_{Hh}(\mathbf{g}))$. To this end we use the identity that follows from the Cauchy-Schwarz inequality in $\mathbb{R}^2$:

$$\max_{\|\mathscr{F}_r^{-1}\boldsymbol{\mu}_{tr}\|\le g_r} (\mathbf{T}_{1r}\mathbf{v},\mathbf{T}_{2r}\mathbf{v})\boldsymbol{\mu}_{tr} = g_r\|\mathscr{F}_r(\mathbf{T}_{1r}\mathbf{v},\mathbf{T}_{2r}\mathbf{v})^\top\|, \tag{12}$$

where $\boldsymbol{\mu}_{tr} := (\mu_{t_1 r},\mu_{t_2 r})^\top \in \mathbb{R}^2$, $r=1,\dots,m$, will play the role of the Lagrange multipliers.

In the dual formulation of $(\mathscr{P}_{Hh}(\mathbf{g}))$ we will use four types of the Lagrange multipliers: $\boldsymbol{\mu}_\nu \in \mathbb{R}^m$ releases the non-penetration condition, $\boldsymbol{\mu}_{t_1},\boldsymbol{\mu}_{t_2} \in \mathbb{R}^m$, where $\boldsymbol{\mu}_{t_j} = (\mu_{t_j,1},\dots,\mu_{t_j,m})^\top$, $j=1,2$, regularize the non-differentiable term via (12), $\boldsymbol{\mu}_e \in \mathbb{R}^{m_e}$ glues the subdomains, and $\boldsymbol{\mu}_d \in \mathbb{R}^{m_d}$ enforces the Dirichlet boundary condition be satisfied. To simplify notation we denote

$$\boldsymbol{\mu} := \begin{pmatrix} \boldsymbol{\mu}_\nu \\ \boldsymbol{\mu}_{t_1} \\ \boldsymbol{\mu}_{t_2} \\ \boldsymbol{\mu}_e \\ \boldsymbol{\mu}_d \end{pmatrix}, \quad \mathbf{B} := \begin{pmatrix} \mathbf{N} \\ \mathbf{T}_1 \\ \mathbf{T}_2 \\ \mathbf{B}_e \\ \mathbf{B}_d \end{pmatrix}, \quad \mathbf{c} := \begin{pmatrix} \mathbf{d} \\ \mathbf{0} \\ \mathbf{0} \\ \mathbf{0} \\ \mathbf{0} \end{pmatrix}.$$

Then the Lagrangian corresponding to $(\mathscr{P}_{Hh}(\mathbf{g}))$ reads as follows:

$$L(\mathbf{v},\boldsymbol{\mu}) := \frac{1}{2}\mathbf{v}^\top\mathbf{K}\mathbf{v} - \mathbf{v}^\top\mathbf{f} + \boldsymbol{\mu}^\top(\mathbf{B}\mathbf{v}-\mathbf{c}), \quad (\mathbf{v},\boldsymbol{\mu}) \in \mathbb{R}^n \times \boldsymbol{\Lambda}(\mathbf{g}),$$

where the set of the Lagrange multipliers is given by

$$\boldsymbol{\Lambda}(\mathbf{g}) := \{\boldsymbol{\mu} \in \mathbb{R}^{3m+m_e+m_d} : \mu_{\nu r} \ge 0, \|\mathscr{F}_r^{-1}\boldsymbol{\mu}_{tr}\|^2 \le g_r^2, r=1,\dots,m\}.$$

It is well-known that the solution to $(\mathscr{P}_{Hh}(\mathbf{g}))$ is the first component of the solution to the following *saddle-point problem*:

$$\left.\begin{aligned} &\textit{Find } (\mathbf{u},\boldsymbol{\lambda}) \in \mathbb{R}^n \times \boldsymbol{\Lambda}(\mathbf{g}) \textit{ such that} \\ &L(\mathbf{u},\boldsymbol{\lambda}) = \min_{\mathbf{v}\in\mathbb{R}^n}\max_{\boldsymbol{\mu}\in\boldsymbol{\Lambda}(\mathbf{g})} L(\mathbf{v},\boldsymbol{\mu}) = \max_{\boldsymbol{\mu}\in\boldsymbol{\Lambda}(\mathbf{g})}\min_{\mathbf{v}\in\mathbb{R}^n} L(\mathbf{v},\boldsymbol{\mu}). \end{aligned}\right\} \qquad (\mathscr{S}_{Hh}(\mathbf{g}))$$

As the Lagrangian L is convex in the first variable, the solution to $(\mathscr{S}_{Hh}(\mathbf{g}))$ necessarily satisfies the stationarity condition:

$$\frac{\partial L}{\partial \mathbf{v}}(\mathbf{u},\boldsymbol{\lambda}) = \mathbf{0} \quad \Longleftrightarrow \quad \mathbf{K}\mathbf{u} - \mathbf{f} + \mathbf{B}^\top\boldsymbol{\lambda} = \mathbf{0}.$$

The last equation is fulfilled iff

$$\mathbf{f}-\mathbf{B}^\top\boldsymbol{\lambda}\in Im\,\mathbf{K} \tag{13}$$

and

$$\mathbf{u}=\mathbf{K}^\dagger(\mathbf{f}-\mathbf{B}\boldsymbol{\lambda})+\mathbf{R}\boldsymbol{\alpha} \tag{14}$$

for an appropriate $\boldsymbol{\alpha}\in\mathbb{R}^{6(s_1+s_2)}$. Let us note that $\boldsymbol{\alpha}$ can be computed solely from $\boldsymbol{\lambda}$ when $\boldsymbol{\lambda}$ is known [13].

Since $Ker\,\mathbf{K}$ is the orthogonal complement of $Im\,\mathbf{K}$ in $\mathbb{R}^n$, one can write (13) equivalently as

$$\mathbf{R}^\top(\mathbf{f}-\mathbf{B}^\top\boldsymbol{\lambda})=\mathbf{0}. \tag{15}$$

Eliminating $\mathbf{u}$ from $(\mathscr{S}_{Hh}(\mathbf{g}))$ by using (14) and adding the constraint (15) to the definition of the set of the Lagrange multipliers we arrive at the *dual problem*:

$$\textit{Find } \boldsymbol{\lambda}\in\boldsymbol{\Lambda}^{\#}(\mathbf{g}) \textit{ such that } D(\boldsymbol{\lambda})=\min_{\boldsymbol{\mu}\in\boldsymbol{\Lambda}^{\#}(\mathbf{g})}D(\boldsymbol{\mu}), \qquad (\mathscr{D}_{Hh}(\mathbf{g}))$$

where

$$D(\boldsymbol{\mu}):=\frac{1}{2}\boldsymbol{\mu}^\top\mathbf{B}\mathbf{K}^\dagger\mathbf{B}^\top\boldsymbol{\mu}-\boldsymbol{\mu}^\top(\mathbf{B}\mathbf{K}^\dagger\mathbf{f}-\mathbf{c}),$$
$$\boldsymbol{\Lambda}^{\#}(\mathbf{g}):=\{\boldsymbol{\mu}\in\boldsymbol{\Lambda}(\mathbf{g}):\mathbf{R}^\top\mathbf{B}^\top\boldsymbol{\mu}=\mathbf{R}^\top\mathbf{f}\}.$$

To simplify the next presentation we denote:

$$\mathbf{F}:=\mathbf{B}\mathbf{K}^\dagger\mathbf{B}^\top,\ \widetilde{\mathbf{h}}:=\mathbf{B}\mathbf{K}^\dagger\mathbf{f}-\mathbf{c},\ \mathbf{G}:=\mathbf{R}^\top\mathbf{B}^\top,\ \mathbf{e}:=\mathbf{R}^\top\mathbf{f}.$$

Then the solution $\boldsymbol{\lambda}$ to $(\mathscr{D}_{Hh}(\mathbf{g}))$ satisfies (see (15))

$$\mathbf{G}\boldsymbol{\lambda}=\mathbf{e}.$$

Since $\boldsymbol{\lambda}$ can be uniquely decomposed into $\boldsymbol{\lambda}_{Im}\in Im\,\mathbf{G}^\top$ and $\boldsymbol{\lambda}_{Ker}\in Ker\,\mathbf{G}$ as

$$\boldsymbol{\lambda}=\boldsymbol{\lambda}_{Im}+\boldsymbol{\lambda}_{Ker} \tag{16}$$

and $\boldsymbol{\lambda}_{Im}$ is easily computable by

$$\boldsymbol{\lambda}_{Im}=\mathbf{G}^\top(\mathbf{G}\mathbf{G}^\top)^{-1}\mathbf{e},$$

it remains to show how to get $\boldsymbol{\lambda}_{Ker}$. Inserting (16) into $(\mathscr{D}_{Hh}(\mathbf{g}))$ we obtain the new minimization problem for $\boldsymbol{\lambda}_{Ker}$:

$$\textit{Find } \boldsymbol{\lambda}_{Ker}\in\boldsymbol{\Lambda}^{\#}_{Ker}(\mathbf{g}) \textit{ such that } D_{Ker}(\boldsymbol{\lambda}_{Ker})=\min_{\boldsymbol{\mu}\in\boldsymbol{\Lambda}^{\#}_{Ker}(\mathbf{g})}D_{Ker}(\boldsymbol{\mu}), \qquad (\mathscr{D}'_{Hh}(\mathbf{g}))$$

where

$$D_{Ker}(\boldsymbol{\mu}):=\frac{1}{2}\boldsymbol{\mu}^\top\mathbf{F}\boldsymbol{\mu}-\boldsymbol{\mu}^\top\mathbf{h},\quad \mathbf{h}:=\widetilde{\mathbf{h}}-\mathbf{F}\boldsymbol{\lambda}_{Im},$$
$$\boldsymbol{\Lambda}^{\#}_{Ker}(\mathbf{g}):=\{\boldsymbol{\mu}\in\mathbb{R}^{3m+m_e+m_d}:\ \boldsymbol{\mu}+\boldsymbol{\lambda}_{Im}\in\boldsymbol{\Lambda}(\mathbf{g}),\mathbf{G}\boldsymbol{\mu}=\mathbf{0}\}.$$

Finally we apply the orthogonal projectors $\mathbf{Q}$ and $\mathbf{P}$ on $Im\,\mathbf{G}^\top$ and $Ker\,\mathbf{G}$:

$$\mathbf{Q} := \mathbf{G}^\top(\mathbf{G}\mathbf{G}^\top)^{-1}\mathbf{G} \quad \text{and} \quad \mathbf{P} := \mathbf{I} - \mathbf{Q},$$

respectively. It is easy to verify that $(\mathscr{D}'_{Hh}(\mathbf{g}))$ is equivalent to:

$$\textit{Find } \boldsymbol{\lambda}_{Ker} \in \boldsymbol{\Lambda}^{\#}_{Ker}(\mathbf{g}) \textit{ such that } D^{Proj}_{Ker}(\boldsymbol{\lambda}_{Ker}) = \min_{\boldsymbol{\mu}\in\boldsymbol{\Lambda}^{\#}_{Ker}(\mathbf{g})} D^{Proj}_{Ker}(\boldsymbol{\mu}), \qquad (\mathscr{D}''_{Hh}(\mathbf{g}))$$

where

$$D^{Proj}_{Ker}(\boldsymbol{\mu}) := \frac{1}{2}\boldsymbol{\mu}^\top(\mathbf{PFP}+\rho\mathbf{Q})\boldsymbol{\mu} - \boldsymbol{\mu}^\top\mathbf{Ph}, \quad \rho > 0.$$

Let us denote the Hessian of the quadratic form D^{Proj}_{Ker} by $\mathbf{A}_\rho$, i.e.,

$$\mathbf{A}_\rho := \mathbf{PFP} + \rho\mathbf{Q}.$$

Before proving the bounds on the spectrum of $\mathbf{A}_\rho$ we introduce several auxiliary results. Let us note that the Moore-Pensrose inverse $\mathbf{K}^\dagger$ plays the key role in the proofs.

Lemma 2. PFP *is non-singular on* $Ker\,\mathbf{G}$.

Proof. Since **PFP** is symmetric, positive semi-definite, it is enough to show that its smallest eigenvalue on $Ker\,\mathbf{G}$ is positive. We have:

$$\begin{aligned}
\lambda_{\min}(\mathbf{PFP}|Ker\,\mathbf{G}) &= \min_{\substack{\boldsymbol{\mu}\in Ker\,\mathbf{G}\\ \boldsymbol{\mu}\neq\mathbf{0}}} \frac{\boldsymbol{\mu}^\top\mathbf{PFP}\boldsymbol{\mu}}{\boldsymbol{\mu}^\top\boldsymbol{\mu}} = \min_{\substack{\mathbf{R}^\top\mathbf{B}^\top\boldsymbol{\mu}=\mathbf{0}\\ \boldsymbol{\mu}\neq\mathbf{0}}} \frac{\boldsymbol{\mu}^\top\mathbf{B}\mathbf{K}^\dagger\mathbf{B}^\top\boldsymbol{\mu}}{\boldsymbol{\mu}^\top\boldsymbol{\mu}} = \\
&= \min_{\substack{\mathbf{R}^\top\mathbf{v}=\mathbf{0}\\ \mathbf{v}=\mathbf{B}^\top\boldsymbol{\mu}\\ \boldsymbol{\mu}\neq\mathbf{0}}} \frac{\mathbf{v}^\top\mathbf{K}^\dagger\mathbf{v}}{\mathbf{v}^\top\mathbf{v}} \cdot \frac{\boldsymbol{\mu}^\top\mathbf{B}\mathbf{B}^\top\boldsymbol{\mu}}{\boldsymbol{\mu}^\top\boldsymbol{\mu}} \geq \\
&\geq \min_{\substack{\mathbf{v}\in Im\,\mathbf{K}\cap Im\,\mathbf{B}^\top\\ \mathbf{v}\neq\mathbf{0}}} \frac{\mathbf{v}^\top\mathbf{K}^\dagger\mathbf{v}}{\mathbf{v}^\top\mathbf{v}} \cdot \min_{\substack{\boldsymbol{\mu}\in Ker\,\mathbf{G}\\ \boldsymbol{\mu}\neq\mathbf{0}}} \frac{\boldsymbol{\mu}^\top\mathbf{B}\mathbf{B}^\top\boldsymbol{\mu}}{\boldsymbol{\mu}^\top\boldsymbol{\mu}}.
\end{aligned}$$

Further

$$\min_{\substack{\boldsymbol{\mu}\in Ker\,\mathbf{G}\\ \boldsymbol{\mu}\neq\mathbf{0}}} \frac{\boldsymbol{\mu}^\top\mathbf{B}\mathbf{B}^\top\boldsymbol{\mu}}{\boldsymbol{\mu}^\top\boldsymbol{\mu}} = \lambda_{\min}(\mathbf{B}\mathbf{B}^\top|Ker\,\mathbf{G}) \geq \lambda_{\min}(\mathbf{B}\mathbf{B}^\top) > 0$$

using that $\mathbf{B}$ has the full row rank. From the well-known property of the Moore-Penrose inverse $\mathbf{K}^\dagger$ we get

$$\min_{\substack{\mathbf{v}\in Im\,\mathbf{K}\cap Im\,\mathbf{B}^\top\\ \mathbf{v}\neq\mathbf{0}}} \frac{\mathbf{v}^\top\mathbf{K}^\dagger\mathbf{v}}{\mathbf{v}^\top\mathbf{v}} \geq \min_{\substack{\mathbf{v}\in Im\,\mathbf{K}\\ \mathbf{v}\neq\mathbf{0}}} \frac{\mathbf{v}^\top\mathbf{K}^\dagger\mathbf{v}}{\mathbf{v}^\top\mathbf{v}} = \lambda_{\min}(\mathbf{K}^\dagger|Im\,\mathbf{K}) > 0.$$

Therefore

$$\lambda_{\min}(\mathbf{PFP}|Ker\,\mathbf{G}) \geq \lambda_{\min}(\mathbf{K}^{\dagger}|Im\,\mathbf{K})\lambda_{\min}(\mathbf{B}\mathbf{B}^{\top}|Ker\,\mathbf{G}) > 0$$

that proves the lemma. □

Remark 2. It is easily seen from the proof of Lemma 2 that $\lambda_{\min}(\mathbf{PFP}|Ker\,\mathbf{G}) = 0$ if the requirement on the full row rank of $\mathbf{B}$ is not satisfied.

Lemma 3. *$\mathbf{A}_\rho$ is non-singular on $\mathbb{R}^{3m+m_e+m_d}$. Moreover all non-zero eigenvalues of $\mathbf{PFP}$ are also the eigenvalues of $\mathbf{A}_\rho$ and the remaining eigenvalues of $\mathbf{A}_\rho$ are equal to ρ.*

Proof. As $\mathbf{Q}$, $\mathbf{P}$ are the orthogonal projectors on $Im\,\mathbf{G}^{\top}$ and $Ker\,\mathbf{G}$, respectively, we have $Im(\mathbf{A}_\rho|Im\,\mathbf{G}^{\top}) = Im\,\mathbf{G}^{\top}$ and from Lemma 2 we get $Im(\mathbf{A}_\rho|Ker\,\mathbf{G}) = Ker\,\mathbf{G}$. Therefore $Im\,\mathbf{G}^{\top}$ and $Ker\,\mathbf{G}$ are the invariant subspaces of $\mathbf{A}_\rho$ in $\mathbb{R}^{3m+m_e+m_d}$. The assertions follows from the fact that $\mathbf{PFP}$ vanishes on $Im\,\mathbf{G}^{\top}$ while $\rho\mathbf{Q}$ vanishes on $Ker\,\mathbf{G}$. □

Corollary 1. Let $\rho = \rho_0\lambda_{\max}(\mathbf{PFP}|Ker\,\mathbf{G})$ with $\rho_0 > 0$. Then from Lemma 3 it follows:

$$\kappa(\mathbf{A}_\rho) = \begin{cases} \rho_0\kappa(\mathbf{PFP}|Ker\,\mathbf{G}) & \text{for } \rho_0 > 1, \\ \kappa(\mathbf{PFP}|Ker\,\mathbf{G}) & \text{for } \rho_0 \in [\kappa(\mathbf{PFP}|Ker\,\mathbf{G})^{-1}, 1], \\ \rho_0^{-1} & \text{for } \rho_0 < \kappa(\mathbf{PFP}|Ker\,\mathbf{G})^{-1}. \end{cases}$$

Thus the smallest value of the spectral condition number of $\mathbf{A}_\rho$ is $\kappa(\mathbf{PFP}|Ker\,\mathbf{G})$.

Theorem 2. *Let $\rho = \lambda_{\max}(\mathbf{PFP}|Ker\,\mathbf{G})$ and let $\mathbf{B}$ be orthogonal. Then*

$$c_2^{-1}\frac{h}{H} \leq \lambda_{\min}(\mathbf{A}_\rho) \quad \textit{and} \quad \lambda_{\max}(\mathbf{A}_\rho) \leq c_1^{-1}\frac{H}{h}, \tag{17}$$

where $c_1 > 0$, $c_2 > 0$ are the same constants as in Assumption 1.

Proof. For our choice of ρ Lemma 3 yields

$$\lambda_{\min}(\mathbf{A}_\rho) = \lambda_{\min}(\mathbf{PFP}|Ker\,\mathbf{G}) \quad \text{and} \quad \lambda_{\max}(\mathbf{A}_\rho) = \lambda_{\max}(\mathbf{PFP}|Ker\,\mathbf{G}).$$

In the proof of Lemma 2 we have found that

$$\lambda_{\min}(\mathbf{PFP}|Ker\,\mathbf{G}) \geq \lambda_{\min}(\mathbf{K}^{\dagger}|Im\,\mathbf{K})\lambda_{\min}(\mathbf{B}\mathbf{B}^{\top}|Ker\,\mathbf{G}).$$

Analogously, the following upper bound can be derived for the maximal eigenvalue:

$$\lambda_{\max}(\mathbf{PFP}|Ker\,\mathbf{G}) \leq \lambda_{\max}(\mathbf{K}^{\dagger}|Im\,\mathbf{K})\lambda_{\max}(\mathbf{B}\mathbf{B}^{\top}|Ker\,\mathbf{G}).$$

Combining these results with (10) and $\mathbf{B}\mathbf{B}^{\top} = \mathbf{I}$ we arrive at (17). □

Remark 3. The assumption on orthogonality of $\mathbf{B}$ simplifies the bounds in (17). In the next section we will use

$$\|\mathbf{G}\| \leq 1 \tag{18}$$

that follows from orthogonality of $\mathbf{B}$ and $\mathbf{R}$.

Remark 4. The analysis in [7, 1] shows that it possible to derive the lower bound in (17) independent of $\frac{h}{H}$ (with a different constant).

5 Algorithms

In this section we introduce the algorithm (in a sense optimal) for solving $(\mathscr{D}''_{Hh}(\mathbf{g}))$, which is based on the augmented Lagrangian method and called the SMALSE-M (semimonotonic augmented Lagrangians for separable and equality constraints; see [4] for more details).

Introducing the new Lagrange multiplier vector $\boldsymbol{\beta} \in \mathbb{R}^{6(s_1+s_2)}$ for the equality constraint in $\boldsymbol{\Lambda}^{\#}_{Ker}(\mathbf{g})$, the augmented Lagrangian to the problem $(\mathscr{D}''_{Hh}(\mathbf{g}))$ reads as follows:

$$L_\rho(\boldsymbol{\mu},\boldsymbol{\beta}) = \frac{1}{2}\boldsymbol{\mu}^\top \mathbf{A}_\rho \boldsymbol{\mu} - \boldsymbol{\mu}^\top \mathbf{P}\mathbf{h} + \boldsymbol{\beta}^\top \mathbf{G}\boldsymbol{\mu}.$$

Our algorithm generates two sequences $\{\boldsymbol{\mu}^{(k)}\}$ and $\{\boldsymbol{\beta}^{(k)}\}$ which approximate $\boldsymbol{\lambda}_{Ker}$ and $\boldsymbol{\beta}$, respectively. Each $\boldsymbol{\mu}^{(k)}$ is computed by

$$\text{minimize } L_\rho(\boldsymbol{\mu},\boldsymbol{\beta}^{(k)}) \quad \text{subject to } \boldsymbol{\mu}+\boldsymbol{\lambda}_{Im} \in \boldsymbol{\Lambda}(\mathbf{g}) \tag{19}$$

for $\boldsymbol{\beta}^{(k)}$ being fixed. In order to recognize a sufficiently accurate approximation of the minima, we need a suitable optimality criterion. To this end we use the *K-gradient* $\mathbf{g}^K(\boldsymbol{\mu},\boldsymbol{\beta}^{(k)})$ represented by the vector of the KKT-optimality conditions to the problem (19).

ALGORITHM SMALSE-M. Given $\boldsymbol{\beta}^{(0)} \in \mathbb{R}^{6(s_1+s_2)}$, $\varepsilon > 0$, $\rho > 0$, $M_0 > 0$, $\eta > 0$, and $\beta > 1$. Set $k := 0$ and $\varepsilon_1 = \varepsilon\|\mathbf{P}\mathbf{h}\|$.

(Step 1.) Find $\boldsymbol{\mu}^{(k)}$ such that $\boldsymbol{\mu}^{(k)} + \boldsymbol{\lambda}_{Im} \in \boldsymbol{\Lambda}(\mathbf{g})$ and

$$\|\mathbf{g}^K(\boldsymbol{\mu},\boldsymbol{\beta}^{(k)})\| \le \min\{M_k\|\mathbf{G}\boldsymbol{\mu}^{(k)}\|, \eta\}.$$

(Step 2.) If $\|\mathbf{g}^K(\boldsymbol{\mu},\boldsymbol{\beta}^{(k)})\| \le \varepsilon_1$ and $\|\mathbf{G}\boldsymbol{\mu}^{(k)}\| \le \varepsilon_1 M_0\|\boldsymbol{\mu}^{(k)}\|$ return $\boldsymbol{\lambda}_{Ker} := \boldsymbol{\mu}^{(k)}$, else go to Step 3.

(Step 3.) Compute $\boldsymbol{\beta}^{(k+1)} = \boldsymbol{\beta}^{(k)} + \rho\mathbf{G}\boldsymbol{\mu}^{(k)}$.

(Step 4.) Update the precision control M_k as follows: if $k > 0$ and

$$L_\rho(\boldsymbol{\mu}^{(k)},\boldsymbol{\beta}^{(k)}) < L_\rho(\boldsymbol{\mu}^{(k-1)},\boldsymbol{\beta}^{(k-1)}) + \frac{\rho}{2}\|\mathbf{G}\boldsymbol{\mu}^{(k)}\|^2$$

then $M_{k+1} = M_k/\beta$, else $M_{k+1} = M_k$.

(Step 5.) Set $k := k+1$ and go to Step 1.

Step 1 can be performed by the *K-convergent* algorithm for solving (19), i.e., the algorithm that guarantees convergence of the K-gradient $\mathbf{g}^K$ to zero [4]. As (19) is a minimization problem for the strictly convex quadratic function with the separable convex constraints, we use the algorithm proposed in [17] that generalizes ideas

from [5] originally developed for simple bound constraints. The analysis in [18] shows that its convergence rate can be expressed in terms of the spectral condition number of $\mathbf{A}_\rho$. This result together with the analysis in [4] are the important ingredients for the proof of the scalability of the SAMLSE-M if applied to problems $(\mathscr{D}''_{Hh}(\mathbf{g}))$ with a bounded ratio $\frac{H}{h}$. The details of the prove will be presented elsewhere.

Let us return to the problem with Coulomb friction $(\mathscr{P})$. The algebraic counterpart of the mapping $\boldsymbol{\Psi}$ reads as follows:

$$\boldsymbol{\Psi} : \mathbf{g} \mapsto \boldsymbol{\lambda}_\nu, \quad \mathbf{g} \in \mathbb{R}^m_+,$$

where $\boldsymbol{\lambda}_\nu$ is the first subvector in $\boldsymbol{\lambda}$ (solution to $(\mathscr{D}_{Hh}(\mathbf{g}))$) which corresponds to the discrete normal contact stress. A *discrete solution* to the contact problem with Coulomb friction is defined by

$$\boldsymbol{\Psi}(\boldsymbol{\lambda}_\nu) = \boldsymbol{\lambda}_\nu,$$

i.e., $\boldsymbol{\lambda}_\nu$ is a fixed-point of $\boldsymbol{\Psi}$ in $\mathbb{R}^m_+$. To find it one can use the method of successive approximations:

$$\textit{Initialize } \boldsymbol{\lambda}_\nu^{(0)} \in \mathbb{R}^m_+ : \quad \boldsymbol{\lambda}_\nu^{(k+1)} = \boldsymbol{\Psi}(\boldsymbol{\lambda}_\nu^{(k)}), \quad k = 0,1,2,\ldots \tag{20}$$

It is well-known that the sequence $\{\boldsymbol{\lambda}_\nu^{(k)}\}$ generated by (20) converges to the fixed-point $\boldsymbol{\lambda}_\nu$ if $\boldsymbol{\Psi}$ is contractive in $\mathbb{R}^m_+$ and, in addition, such a fixed-point is unique. This property holds provided that the coefficient of friction is small enough [11]. As the evaluation of $\boldsymbol{\Psi}(\boldsymbol{\lambda}_\nu^{(k)})$ requires to solve $(\mathscr{D}_{Hh}(\mathbf{g}))$ with $\mathbf{g} := \boldsymbol{\lambda}_\nu^{(k)}$, we can combine (20) with the SMALSE-M. The most efficient implementation is the inexact one in which the slip bound $\mathbf{g}$ is updated after each iterative step of the SMALSE-M, i.e., in Step 1 we replace $\boldsymbol{\Lambda}(\mathbf{g})$ by $\boldsymbol{\Lambda}(\boldsymbol{\mu}_\nu^{(k-1)} + \boldsymbol{\lambda}_{Im,\nu})$.

6 Numerical Experiments

We use our algorithm for solving contact problems with isotropic Coulomb friction (for orthotropic friction we refer to [13]).

Consider two bricks

$$\Omega^1 = (0,20) \times (0,10) \times (0,10), \quad \Omega^2 = (0,20) \times (0,10) \times (10,20) \quad \text{(in [mm])}$$

made of elastic, isotropic and homogeneous materials characterized by the Lamè constants $\lambda^1 = 2.792e4$ [MPa], $\mu^1 = 2.593e4$ [MPa] (aluminium) $\lambda^2 = 6.360e4$ [MPa], $\mu^2 = 8.301e4$ [MPa] (steel), respectively. The boundaries of Ω^1 and Ω^2 are split as follows:

$$\Gamma_u^1 = \{0\}\times(0,10)\times(0,10), \quad \Gamma_u^2 = \{0\}\times(0,10)\times(10,20),$$
$$\Gamma_c^1 = (0,20)\times(0,10)\times\{10\}, \quad \Gamma_c^2 = \Gamma_c^1,$$
$$\Gamma_p^1 = \partial\Omega^1 \setminus \overline{\Gamma_u^1 \cup \Gamma_c^1}, \qquad \Gamma_p^2 = \Gamma_p^{2,1} \cup \Gamma_p^{2,2} \cup \Gamma_p^{2,3},$$

where $\Gamma_p^{2,1} = \{20\}\times(0,10)\times(10,20)$, $\Gamma_p^{2,2} = (0,20)\times(0,10)\times\{20\}$, and $\Gamma_p^{2,3} = (0,20)\times\{0,10\}\times(10,20)$; see Figure 1. The non-zero density of surface tractions is prescribed only on $\Gamma_p^{2,1}$ and $\Gamma_p^{2,2}$ as follows:

$$p^2 = (1,0,20)^\top \text{ on } \Gamma_p^{2,1}, \quad p^2 = (0,0,-30)^\top \text{ on } \Gamma_p^{2,2} \quad \text{(in [MPa])}.$$

The volume forces are neglected, i.e., $f^k = 0$ in Ω^k, $k = 1,2$. The coefficient of friction is given by $\mathscr{F}_1 = \mathscr{F}_2 = 0.3$ on Γ_c^1.

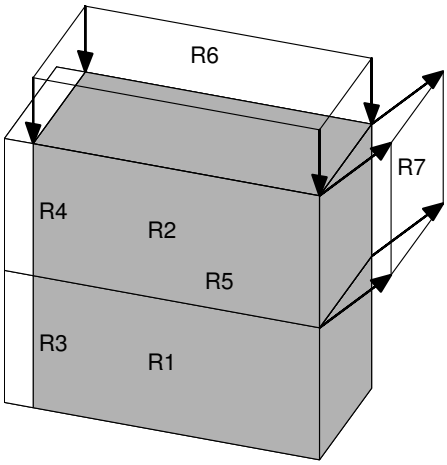

Fig. 1 Geometry of the model problem

Each brick Ω^k, $k = 1,2$, is divided into the same number of sub-domains Ω_H^{ki} represented by bricks of the same size, $i = 1,\ldots,s$, where $s = 2,16,54,128$, and 250. Each Ω_H^{ki} is then decomposed into m_c cubes, $m_c = 8,27,64$, and 125, which are then cut into 5 tetrahedrons creating the partition $\mathscr{T}_{Hh}^{ki}$. These partitions correspond to the ratios $H/h = 2,3,4$, and 5, respectively. We apply the inexact implementation of the method of successive approximations (20) combined with the SMALSE-M as mentioned in Section 5. The following choice of the parameters is used: $\rho := \|\mathbf{PFP}\|$, $\eta := \|\mathbf{Ph}\|$, $\varepsilon := 10^{-5}$, $M_0 := 10^{-6}$, and $\beta := 0.1$. The computations are performed by MatSol system [16] in Matlab R2008b.

Fig. 2 and 3 show the distributions of the normal and tangential contact stress, respectively. It is readily seen that all contact and friction phenomena appear on Γ_c^1 in our model problem, i.e., the slipping and sticking contact zones and the zone of non-contact. In Table 1 we report the numbers of the primal (n), dual variables ($n_d := 3m + m_e + m_d$), and of the rigid body motions ($l := 12s$); the numbers of the

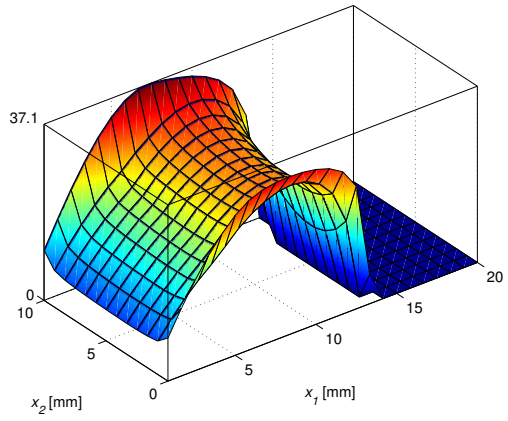

Fig. 2 Negative normal contact stress $-\sigma_\nu$ on Γ_c^1

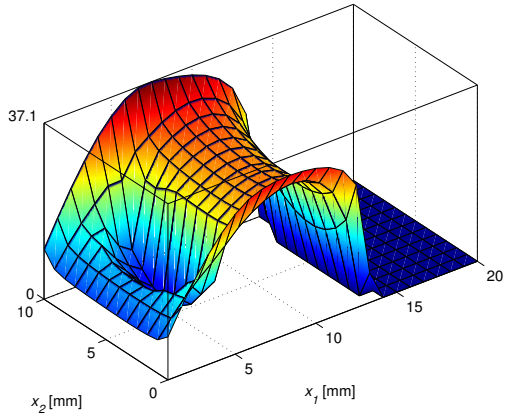

Fig. 3 Scaled norm of the tangential contact stress $\|\mathscr{F}^{-1}\sigma_t\|$ on Γ_c^1. Comparing with Fig. 2 one can detect the non-contact zone by the zero contact stresses. The sticking zone is characterized by different non-zero values of the normal and tangential contact stress. The rest is the slipping zone.

outer iterations (*iter*) and the matrix-vector multiplications (n_{PFP}). In order to assess the relative efficiency we quote the ratio

$$rel_{eff} := \frac{n_{PFP}}{n}.$$

We can see that the computational costs slowly increases for finer meshes but the relative efficiency decreases considerably.

Table 1 Scalability and relative efficiency

$2s$	$H/h=2$	$H/h=3$	$H/h=4$	$H/h=5$
4	(324/153/24) **10/180** *0.5556*	(768/276/24) **10/269** *0.3503*	(1500/435/24) **11/356** *0.2373*	(2592/630/24) **11/470** *0.1813*
32	(2592/1527/192) **11/483** *0.1863*	(6144/2889/192) **11/657** *0.1069*	(12000/4683/192) **11/665** *0.0554*	(20736/6909/192) **12/847** *0.0408*
108	(8748/5493/648) **11/636** *0.0727*	(20736/10506/648) **11/878** *0.0423*	(40500/17139/648) **13/906** *0.0224*	(69984/25392/648) **14/1071** *0.0153*
256	(20736/13419/1536) **12/737** *0.0355*	(49152/25791/1536) **14/939** *0.01910*	(96000/42195/1536) **15/1173** *0.0122*	(165888/62631/1536) **16/1400** *0.0084*
500	(40500/26673/3000) **14/812** *0.0200*	(96000/51408/3000) **15/1039** *0.0108*	(187500/84243/3000) **17/1533** *0.0081*	(324000/125047/3000) **18/1776** *0.0054*

[a] At each position $(n/n_d/l)$, $\boldsymbol{iter/n_{PFP}}$, and rel_{eff} are displayed

7 Conclusions and Comments

We have analyzed the scalable algorithm for solving 3D contact problems with Tresca friction, i.e. the algorithm in which the number of iterations needed to achieve a prescribed accuracy can be independent on the mesh norms. The proof is based on the assumption that the spectrum of the stiffness matrix lies in the fixed interval in $\mathbb{R}^1_+$ when the ratio $\frac{H}{h}$ between the decomposition parameter H and the discretization parameter h is bounded. This assumption is naturally satisfied (at least for regular meshes) when the problems are discretized by the T-FETI domain decomposition method. Another benefit from the T-FETI method is the fact that the kernel space of the stiffness matrix can be identified directly without computations. Therefore we can easily obtain the Moore-Penrose inverse to the stiffness matrix that plays the key role in both the analysis as well as the implementation.

Combining the algorithm for Tresca friction with the method of successive approximations, we can solve contact problems with Coulomb friction. Although the proof of the scalability is an open problem in this case, one can observe it experimentally in numerical tests.

Acknowledgements This research is supported by the project MSM6198910027 of the Ministry of Education of C. R. and by the project GAČR 101/08/0574 of the Grant Agency of C. R.. The paper is partially supported by the IT4Innovations Centre of Excellence project CZ.1.05/1.1.00/02.0070 of the Operational Programme 'Research and Development for Innovations' funded by Structural Funds of E. U. and state budget of C. R..

References

1. Bramble, J.H., Pasciak, J.E., Schatz, A.H.: The construction of preconditioners for elliptic problems by substructuring. I. Math. Comput. **47**, 103-134 (1986)
2. Dostál, Z.: Optimal quadratic programming algorithms: with applications to variational inequalities. Springer, New York (2009)
3. Dostál, Z., Horák, D., Kučera, R.: Total FETI - an easier implementable variant of the FETI method for numerical solution of elliptic PDE. Communications in Numerical Methods in Engineering **22**, 1155–1162 (2006)
4. Dostál, Z., Kučera, R.: An optimal algorithm for minimization of quadratic functions with bounded spectrum subject to separable convex inequality and linear equality constraints. SIAM J. Optimization, **20**, 2913–2938 (2010)
5. Dostál, Z., Schöberl, J.: Minimizing quadratic functions over non-negative cone with the rate of convergence and finite termination. Computational Optimization and Applications **30**, 23–44 (2005)
6. Farhat, C., Lesoinne, M., LeTallec, P., Pierson, K., Rixen, D.: FETI-DP: a dual-primal unified FETI method. I. A faster alternative to the two-level FETI method. Internat. J. Numer. Methods Engrg., **50**, 1523–1544 (2001)
7. Farhat, C., Mandel, J., Roux, F.: Optimal convergence properties of the FETI domain decomposition method. Comput. Methods Appl. Mech. Engrg. **115**, 365-385 (1994)
8. Glowinski, R.: Numerical methods for nonlinear variational problems. Springer Series in Computational Physics, Springer, New York (1984)
9. Golub, G.H., Van Loan, C.F.: Matrix computation. The Johns Hopkins University Press, Baltimore (1996)
10. Hlaváček, I., Haslinger, J., Nečas, J., Lovíšek J.: Numerical solution of variational inequalities. Springer Series in Applied Mathematical Sciences 66, Springer, New York (1988)
11. Haslinger, J.: Approximation of the Signorini problem with friction, obeying Coulomb law. Math. Meth. Appl., **5**, 422–437 (1083)
12. Haslinger, J., Hlaváček, I., Nečas, J.: Numerical methods for for unilateral problems in solid mechanics. In Handbook of Numerical Analysis, vol. IV, Ciarlet, P.G. and Lions, J.L. eds., North-Holland, Amsterdam, 313–485 (1996)
13. Haslinger, J., Kučera, R., Kozubek, T.: Numerical solution of contact problems with orthotropic Coulomb friction based on quadratic programming approach with the elliptic friction cone. Unpublished paper (2011) at http://homel.vsb.cz/∼kuc14/ortho_fric.pdf.
14. Kikuchi, N., Oden, J.T.: Contact problems in elasticity. SIAM, Philadelphia, (1988)
15. Klawonn, A., Widlund, O.B., Dryja, M.: Dual-primal FETI methods for three-dimensional elliptic problems with heterogeneous coefficients. SIAM J. Numer. Anal., **40**, pp. 159–179 (2002)
16. Kozubek, T., Markopoulos, A., Brzobohatý, T., Kučera, R., Vondrák, V., Dostál, Z.: MatSol - MATLAB efficient solvers for problems in engineering. http://www.am.vsb.cz/matsol
17. Kučera, R.: Minimizing quadratic functions with separable quadratic constraints. Optim. Meth. Soft. **22**, 453–467 (2007)
18. Kučera, R.: Convergence rate of an optimization algorithm for minimizing quadratic functions with separable convex constraints. SIAM J. Optim. **19**, 846–862 (2008)
19. Kučera, R., Kozubek, T., Markopoulos, A., Machalová, J.: On the Moore-Penrose inverse in solving saddle-point systems with singular diagonal blocks. Num. Lin. Algebra Appl., **19**, 677–699 (2112).